THE JOURNAL OF BIOLOGICAL CHEMISTRY
Vol. 279, No. 38, Issue of September 17, pp. 39532–39540, 2004

Printed in U.S.A.

Reconstruction and Functional Characterization of the Human Mitochondrial Metabolic Network Based on Proteomic and Biochemical Data*[S]

Received for publication, April 5, 2004, and in revised form, June 2, 2004
Published, JBC Papers in Press, June 17, 2004, DOI 10.1074/jbc.M403782200

Thuy D. Vo‡, Harvey J. Greenberg§, and Bernhard O. Palsson‡¶

From the ‡Department of Bioengineering, University of California, San Diego, California 92093 and the §Department of Mathematics, University of Colorado, Denver, Colorado 80217-3364

Diverse datasets including genomic, proteomic, isotopomer, and DNA sequence variation are becoming available for human mitochondria. Thus there is a need to integrate these data within an *in silico* modeling framework where mitochondrial biology and related disorders can be studied and analyzed. This paper reports a reconstruction and characterization of the human mitochondrial metabolic network based on proteomic and biochemical data. The 189 reactions included in this reconstruction are both elementally and charge-balanced and are assigned to their respective cellular compartments (mitochondrial, cytosol, or extracellular). The capabilities of the reconstructed network to fulfill three metabolic functions (ATP production, heme synthesis, and mixed phospholipid synthesis) were determined. Network-based analysis of the mitochondrial energy conversion process showed that the overall ATP yield per glucose is 31.5. Network flexibility, characterized by allowable variation in reaction fluxes, was evaluated using flux variability analysis and analysis of all of the possible optimal flux distributions. Results showed that the network has high flexibility for the biosynthesis of heme and phospholipids but modest flexibility for maximal ATP production. A subset of all of the optimal network flux distributions, computed with respect to the three metabolic functions individually, was found to be highly correlated, suggesting that this set may contain physiological meaningful fluxes. Examinations of optimal flux distributions also identified correlated reaction sets that form functional modules in the network.

In recent years there has been increasing interest in the mitochondrion as numerous important physiological functions and disorders have been linked to this organelle (1–3). Malfunctioning mitochondrial metabolism is known to play a role not only in rare childhood diseases but also in many leading causes of death including heart disease, diabetes, and Parkinson's disease. The human mitochondrial genome was one of the first genomes to be sequenced (4), and more recently, the proteome of the human cardiac mitochondrion has been identified in two separate studies (5, 6). The analyses of mitochondrial proteomic and isotopomer data have proven to be useful in detecting the onset of cancer and studying glucose homeostasis in diabetes (7, 8). With the increasing availability of these independent datasets, there is a growing need for incorporating and reconciling such information in a genetically and biochemically consistent format. We have developed a constraint-based model of the human cardiac mitochondrion to meet this need.

The constraint-based approach for analyzing reconstructed networks involves the application of a series of constraints arising from reaction stoichiometry, thermodynamics, enzymatic capacities, and regulatory and kinetic constraints when they are available (9, 10). Using this approach, a variety of methods including flux balance analysis (11, 12), extreme pathway analysis (13, 14), and mixed integer linear programming (15) have been developed to characterize the steady-state solution space and search for physiologically relevant metabolic flux distributions. In this paper, optimal flux distributions, alternate optima, extreme points, and optimal solutions are used interchangeably. These terms refer to a set of equivalent paths that the network may use to optimally satisfy a stated metabolic demand. Knowledge about these alternate optima allows one to identify correlated reaction sets that are always used together to carry out a specific biological function (16).

This paper reports an initial reconstruction and characterization of the human mitochondrial metabolic network based on recently published proteomic data (6). The present network describes 189 reactions and 230 metabolites. This reconstruction accounts for energy metabolism, reactive oxygen species (ROS)[1] detoxification, and heme synthesis as well as nitrogen and lipid metabolism. Constraint-based analysis was applied to calculate optimal steady-state flux distributions of the mitochondrial network. Three separate objective functions were used to model three physiological functions of the mitochondria: ATP production, heme biosynthesis, and mixed phospholipid biosynthesis. We further characterized the inherent flexibility of the reconstructed network in carrying out these metabolic functions.

MATERIALS AND METHODS

Constraint-based Modeling—A stoichiometric matrix, $\mathbf{S}$ ($m \times n$), is constructed where m is the number of metabolites and n is the number of reactions in the reconstructed network. A system of mass balance equations for all of the metabolites at steady state is represented as $\mathbf{S}\cdot\mathbf{v} = 0$, where $\mathbf{v}$ is a flux vector (12, 17). Constraints for each reaction have the form $\alpha_i \leq v_i \leq \beta_i$, where α_i and β_i represent the known lower and upper limits of the corresponding reaction flux. The α_i values for irreversible reactions are set to zero, whereas β_i values are usually set to V_{max} of the corresponding enzymes or measured uptake rates for transport reactions. In the absence of V_{max} data or measured uptake rates, the β_i values are set to arbitrary large values. Content and

* This work was supported by the San Diego Fellowship (to T. D. V.). The costs of publication of this article were defrayed in part by the payment of page charges. This article must therefore be hereby marked "*advertisement*" in accordance with 18 U.S.C. Section 1734 solely to indicate this fact.

[S] The on-line version of this article (available at http://www.jbc.org) contains Supplemental data S1–S5.

¶ To whom correspondence should be addressed: Dept. of Bioengineering, 9500 Gilman Dr., P. O. Box 0412, La Jolla, CA 92093-0412. Tel.: 858-534-5668; Fax: 858-822-3120; E-mail: bpalsson@be-research.ucsd.edu.

[1] The abbreviations used are: ROS, reactive oxygen species; OxPhos, oxidative phosphorylation.

TABLE I
Summary of the composition of the mitochondrial metabolic network
The abbreviations used are: C, cytosol; M, mitochondrial matrix; E, extracellular.

	Number of reactions	Compartment
Glycolysis	12	C
Citric acid cycle	10	M
Oxidative phosphorylation	6	M
ROS detoxification	9	C, M
Fatty acid oxidation	31	M
Phospholipid biosynthesis	16	M
Urea cycle	8	C, M
Porphyrin biosynthesis	12	C, M
Transport and others	85	C, M, E
Total network	189	C, M, E

specific constraints on reactions in this network are listed in Tables I–III and Supplemental data S1–S2.

Linear programming was used to find a flux distribution that maximizes a particular objective function (18). The three objective functions considered for the mitochondrial network are listed in Table II. The first objective function is written as an ATP hydrolysis reaction, so that the network can recycle ADP and phosphate. The coefficients in the second objective function are derived from the phospholipid composition of the mitochondria (19–21). The last objective function is simply the production of protoheme. Network reconstruction and flux balance analysis were done using the software package SimPheny (22).

Flux Variability Analysis—To explore the flexibility of individual reaction fluxes in the network, we set the physiological objective functions (Table II) to their respective optimal values and then maximized and minimized the flux through each reaction in the network (16). For a particular calculation, one of the three physiological objective functions is set to its optimal value; the other two are set to zero. Two linear programming problems (maximizing and minimizing) are solved for each reaction in the network. All of the other constraints regarding mass balance, reversibility, and enzymatic capacity are kept the same.

Thermodynamically infeasible cycles, identified using the extreme pathway algorithm (23), in the network have no net flux (16, 24). Because these cycles are never used *in vivo*, we removed one reversible reaction from the cycle such that it would not disconnect any metabolite from the rest of the network. For this study, two reactions (ORNt3m and CITRtm) were removed for this purpose. All of the calculations for flux variability analysis were implemented in GAMS using the CPLEX solver (25) and independently checked with the Mosek solver (26).

Identification of Alternate Optima—Current linear programming solvers do not have the ability to provide alternate optima automatically. This must be done after finding one optimal extreme point and executing a vertex-enumeration algorithm. Lee *et al.* (15) use mixed integer programming to perform this task. We developed an alternative method using MATLAB (27) as the main host, Mosek (26) as the linear programming solver, and *lrs* (28, 29) as the extreme point enumeration program. The algorithm to enumerate all of the alternate optima involves the following three steps.

1) A linear programming formulation of the stoichiometric matrix, constraints, and objective functions as described in the constraint-based modeling section was implemented in MATLAB: max $\{Z = c^T v: \mathbf{S}\cdot\mathbf{v} = 0, \alpha_i \leq v_i \leq \beta_i\}$, where **S** is the stoichiometric matrix, **v** is the flux vector, **c** corresponds to one of the three objective functions listed in Table II, and α_i and β_i are the respective upper and lower bounds on the reaction flux v_i. Mosek, an optimization system available for use with MATLAB interface, was applied to solve this linear programming problem for an initial optimal extreme point $\mathbf{v}^0$.

2) To reduce the dimension of the problem, reactions that must have a fixed flux value (identified from flux variability analysis) were considered to be constants. To enumerate only basic optimal flux distributions, we imposed $\mathbf{c^T v} = Z^*$, where $Z^* = \mathbf{c^T v}^0$ as an additional constraint.

3) The set of inequalities of the optimal solution space, $F^* = \{\mathbf{v} \in$ Feasible solution space: $\mathbf{c^T v} = Z^*\}$, were then passed to *lrs* to obtain its corresponding vertex representation (and hence its number of extreme points). Because *lrs* requires the origin to be an extreme point, we translated F* to the one computed extreme point, $\mathbf{v}^0$, to obtain a set of change vectors: $D = \{\mathbf{d}: \mathbf{v}^0 + \mathbf{d}$ in $F^*\}$. Thus if $\{\mathbf{d}^k\}$ is an extreme point of D, $\{\mathbf{v}^0 + \mathbf{d}^k\}$ is an extreme point of F*.

The MATLAB collection of scripts and functions that executes the above algorithm is available upon request. Details of how *lrs* enumerates the extreme points can be found in the Refs. 28 and 29. It should be noted that, although this method works well here, tighter bounds may cause a combinatorial explosion in the number of extreme points, making complete enumeration impractical.

TABLE II
Metabolic objective functions used in the analysis of the mitochondrial network

ATP production	$Z = -1$ ATP -1 H_2O + 1 ADP + 1 P_i + 1 H^+
Phospholipid biosynthesis	Z = 0.18 cardiolipin + 0.34 phosphatidylethanolamine + 0.43 phosphatidylcholine
Heme biosynthesis	Z = protoheme

Multiple Objective Analysis—The three objective functions can be considered simultaneously by using the concept of "Pareto optimality." A feasible flux **v** is dominated by another feasible flux **v**′ if $f_i(v') \geq f_i(v)$ for all of the objective functions, $\{f_i\}$, and $f_i(v') > f_i(v)$ for at least one f_i. A feasible flux is Pareto optimal if it is not dominated by any other feasible flux. The set of Pareto optimal fluxes is called the "efficient frontier."

Two methods to compute Pareto optima are weights and lexicography. The weight formulation allows one to designate a composite objective function that includes all three mitochondrial functions, each weighed by a positive coefficient, w_i. All of the members of the efficient frontier can be found by maximizing an associated weighted sum: $\Sigma_i w_i f_i(v)$, where the weight vector $w > 0$. Alternatively, we can hierarchically order the objectives and solve a succession of optimization problems. The ordering gives a "lexicographic-max" of the vector $f = (f_1, f_2,$ and $f_3)$. In our case, we order the objectives such that f_1 = ATP demand, f_2 = heme, and f_3 = phospholipids, and solve three linear programming problems as shown in Equations 1–3. The fluxes in the last optimal set are Pareto optimal.

$$f^*_1 = \max\{c^T_{ATP} v: \mathbf{S}\cdot v = 0, \alpha_i \leq v_i \leq \beta_i\} \quad \text{(Eq. 1)}$$

$$f^*_2 = \max\{c^T_{Heme} v: \mathbf{S}\cdot v = 0, \alpha_i \leq v_i \leq \beta_i, c^T_{ATP} v = f^*_1\} \quad \text{(Eq. 2)}$$

$$f^*_3 = \max\{c^T_{Phos} v: \mathbf{S}\cdot v = 0, \alpha_i \leq v_i \leq \beta_i, c_{ATP} v = f^*_1, c^T_{Heme} v = f^*_2\} \quad \text{(Eq. 3)}$$

Correlated Reaction Sets—Equivalent optimal solutions are grouped together to form a matrix (**P**), where rows correspond to different reactions and columns represent different optimal solutions. A binary form of this matrix (**B**) was created such that $\mathbf{B}_{ij}$ has value zero, where $\mathbf{P}_{ij}$ is zero (or lower than the tolerance value of 0.0001) and one otherwise. Diagonal elements of the resulting participation matrix ($\mathbf{BB^T}$) correspond to the number of alternate optima in which these reactions participate (participation number). The correlated reaction sets can be determined by joining reactions that have the same participation number in each row of $\mathbf{BB^T}$ (30).

RESULTS

Based on proteomic and biochemical data, we first reconstructed the most comprehensive metabolic network available for the human mitochondrion to date. Second, we determined the capabilities of the reconstructed network to maximally fulfill three different metabolic functions: ATP production, heme production, and mixed phospholipid production. Third, we assessed the network flexibility (16) in individually satisfying these three metabolic functions by calculating the allowable flux range in each reaction. Fourth, we calculated equivalent optimal flux distributions (15, 31) in the network with respect to each metabolic objective and identified flux distributions that satisfy all three metabolic functions. Lastly, we identified correlated reaction sets (30) that likely form functional modules in the network.

Composition of the Mitochondrial Metabolic Network—The most complete catalog of the mitochondrial proteome to date identified 615 proteins, of which 298 were assigned to 153 unique enzymatic reactions (6) in the human cardiac myocyte. Since the cataloged proteome may be incomplete (32), metabolic reactions catalyzed by enzymes found in the proteome were augmented with biochemical data from the primary liter-

TABLE III
Constraints on reaction fluxes in the network

These data were collected primarily from experiments with rat heart and liver mitochondria. Please refer to the Supplemental data S1 for abbreviations of reactions and metabolites. The symbols [m] and [c] at the beginning of a reaction indicate whether the reaction occurs inside the mitochondria or cytosol, respectively. The [m] and [c] following a metabolite denote the compartmental location of that metabolite. LB and UB represent lower bound and upper bound on reaction fluxes, respectively. All of the data below have the units of μmol/min/g proteins, which were converted from reported units as necessary. Most of the references do not specify whether the reported unit is "g total mitochondrial proteins" or "g isolated proteins." We decided that "g total mitochondrial proteins" is more appropriate based on the reported experimental procedures.

Reactions	Equations	LB	UB	References
CRNtim	crn[m] → crn[c]	0	200	(57)
C160CPT2	[m]: coa + pmtcrn → crn + pmtcoa	0	475	(58)
C160CPT1	[c]: crn + pmtcoa → coa + pmtcrn	0	468	(58)
ASPGLUm	asp-L[m] + glu-L[c] + h[c] ↔ asp-L[c] + glu-L[m] + h[m]	−40	93	(59)
PDHm	[m]: coa + nad + pyr → accoa + co2 + nadh	0	32	(60)
MALtm	mal-L[c] + pi[m] ↔ mal-L[m] + pi[c]	−20	19	(61)
CITtbm	cit[c] + pep[m] ↔ cit[m] + pep[c]	−104	104	(62)
PYRt2m	h[c] + pyr[c] ↔ h[m] + pyr[m]	−110	110	(60)
CITtam	cit[c] +mal-L[m] ↔ cit[m] + mal-L[c]	−92	113	(62)
SUCCt2m	pi[m] + succ[c] ↔ pi[c] + succ[m]	−13	13	(63)
LYStm	h[m] + lys-L[c] ↔ h[c] + lys-L[m]	−120	120	(64)
ARGtm	arg-L[c] + h[m] ↔ arg-L[m] + h[c]	−105	105	(64)
CITRtm	citr-L[m] ↔ citr-L[c]	−60	60	(64)
ATPtm	adp[c] + atp[m] → adp[m] + atp[c]	−33	33	(65)
ORNt4m	citr-L[c] + h[c] + orn[m] ↔ citr-L[m] + h[m] + orn[c]	−150	150	(64)

ature to form an initial reconstruction of the human mitochondrial metabolic network. This network is comprised of 189 reactions and 230 metabolites in three cellular compartments. The included reactions describe the citric acid cycle, oxidative phosphorylation (OxPhos), fatty acid β-oxidation, phospholipid biosynthesis, urea cycle, and ROS detoxification. Glycolytic reactions were also included, because they were identified in the mitochondrial proteome and appeared to be physically associated with the mitochondria (33). Reaction maps and the complete content of the network can be found in the Supplemental data S1–S2 and S5A.

Every metabolite and reaction in the network are localized to a cellular compartment. The three compartments included in the model are the mitochondrial matrix, the cytosol, and the extracellular space. These compartments contain 120, 87, and 23 metabolites, respectively. The mitochondrial intermembrane compartment is not explicitly accounted for, because most metabolites under 10 kDa freely travel across the outer mitochondrial membrane and therefore are considered to be in equilibrium with the cytosol (34). Metabolites are also characterized by their molecular formulas and predominant charge forms determined at pH 7.2. Thus each reaction is elementally and charge balanced.

Each reaction in the network was assigned a "confidence level," which is a measure of how well the data support the existence of that particular reaction. We employed a four-level system for evaluating the confidence level (Table IV). The criteria for each level are as follows: "4" for direct biochemical data; "3" for genetic or proteomic data; "2" for sequence homology or physiological data; and "1" for data based solely on *in silico* arguments. The present reconstruction contains 88 reactions annotated with level 4, 40 with level 3, 31 with level 2, and 30 with level 1. We used level 1 to denote lumped reactions and exchange reactions between the cytosol and the extracellular space.

Capabilities of the Mitochondrial Network—Previous *in silico* studies of mitochondrial metabolism (35–38) primarily focused on energy metabolism, although it is well known that the mitochondrion plays important roles in many cellular processes. The present reconstruction is more comprehensive and therefore can be used to assess a broader range of the physiological functions of the mitochondria. Three metabolic roles are considered in this study: ATP production, heme biosynthesis, and phospholipid biosynthesis. Reactions participating in ROS detoxification and urea metabolism are implicitly considered, because they must be active in order for the network to achieve functional states for the selected metabolic objectives.

Energy Conversion—Normal well perfused myocardium generates >90% of its ATP by oxidative phosphorylation and <10% by glycolysis (39). Most of this ATP is generated by aerobic metabolism taking place in mitochondria; therefore, the efficiency of ATP production within the mitochondrial network is vitally important. We used the reconstructed network to study the ATP yield from three energy sources: glucose, fatty acids, and amino acids.

Glucose Metabolism—The maximal ATP yield per glucose of the reconstructed network is 31.5. This number has been a topic of discussion for many years with some textbooks reporting a value of 36–38 ATP/glucose (34), whereas others report a value of 31 (40, 41). Because all of the reactions in the present reconstruction account for every proton consumed and produced, it was possible to calculate this ATP yield on a network-wide basis. It was found that after accounting for all of the protons consumed in glycolysis, the malate/asparate (Mal/Asp) shuttle, and phosphate transport, there is a net difference of two protons per glucose molecule between our calculations and those reported previously (40, 41). These two protons account for the 0.5 ATP discrepancy. Closer examinations revealed that glycolysis produces a net gain of two protons in the cytosol. These protons may or may not contribute to the proton gradient, which is localized to the mitochondrial intermembrane space, depending on how proximal glycolytic enzymes are to the mitochondria. Since the proteomic data from Taylor *et al.* (6) and other studies (33) have shown that glycolytic enzymes are always found in purified mitochondria samples, it is likely that glycolysis is taking place near the mitochondria and thus the additional proton contribution is significant.

Fatty Acid Metabolism—Cardiac mitochondria derive the majority of their energy from fatty acids (42). Long-chain fatty acids are transported to the mitochondrial matrix by the carnitine shuttle for β-oxidation. Six types of fatty acids (palmitate, stearate, oleate, octadecynoate, arachidonate, and docosahexaenoate) are considered in the present reconstruction. These fatty acids make up 90% of the fatty acid composition of human heart phospholipids (19, 43). Only the ATP yield from palmitate is computed here for comparison with existing literature calculations. The remaining long-chain fatty acids are generally not used for energy but are important in the assem-

TABLE IV
Examples and guidelines for evaluating the confidence level of reactions in the mitochondrial network

Level	Data	Example	Reason
4	Biochemical	Citrate synthase	The enzyme has been purified and characterized, but a reported crystal structure is not required. The mechanism and/or kinetics of the enzymatic reaction have been shown.
3	Genetic or proteomic	Inorganic pyrophosphatase	The gene has been isolated, and the corresponding protein was found in mitochondrial proteome but the mechanism of the catalysis is not well understood. A level of 3 was also assigned to genes/proteins that had biochemical data but were from tissues other than cardiac.
2	Physiological or sequence homology	Pyruvate transport to the mitochondria	Activity of the enzyme has been observed, but no gene has been identified.
1	*In silico*	Glycerol transport	There has been no documentation on glycerol being transported from the extracellular space to the cytosol. It is possible that glycerol is also produced in the cytosol itself, but the biosynthesis of this molecule is outside the scope of this reconstruction. This reaction is included, because the presence of glycerol is required for the reconstructed mitochondrial network to produce phospholipids.

bly of mitochondrial phospholipids. The maximal ATP yield for each palmitate in the reconstructed network was found to be 106. Biochemistry textbooks usually report a value of 129 ATP (44) or 106 (41) depending on whether NADH is considered to have a P/O ratio of 3 or 2.5, respectively. The P/O ratio refers to the number of ATP molecules produced per pair of electrons donated to the electron transport chain. In our calculations, instead of directly imposing a fixed P/O ratio, we specified the number of protons transported by the electron transport chain and consumed by ATP synthase based on the stoichiometry of these reactions. This result showed that a P/O ratio of 2.5 is consistent with the reconstructed network.

Amino Acid Metabolism—Amino acids can also be catabolized for energy. The metabolism of glutamate is considered here as a representative, because it is formed as an intermediate in the breakdown of many other amino acids. Metabolism of each glutamate produces maximally 20.5 molecules of ATP and generates ammonia, which must be converted to urea for excretion. Note that, although urea production is not a primary function of heart mitochondria, a functional urea cycle is important for amino acid metabolism, which is carried out by most cells in the body.

Heme Biosynthesis—In addition to energy conversion, heme biosynthesis is another function that is common to mitochondria of all of the tissues (45). Heme molecules play an essential role in the assembly of many apoproteins including the electron transfer complexes and catalase. Cytochromes are examples of biologically active hemes that are linked to polypeptides. Only the synthesis of protoheme was considered in the reconstruction, since it has been reported that the synthesis rate of "mature" heme (for example, hemes a and b) is controlled by that of protoheme (46). The carbon backbone of protoheme is derived from succinyl-CoA and glycine. Given the constraints on the network, we found that glycine has a higher shadow price than succinyl-CoA. The shadow price of a metabolite reflects how sensitive the value of the objective function is with respect to that metabolite (47). This finding confirms the experimental results with isolated perfused rat hearts (46), which showed that changes in glycine concentration and uptake rate account for changes in the rate of heme biosynthesis.

Phospholipid Biosynthesis—Mitochondria are semi-autonomous organelles. Besides producing energy and various metabolites for the cells, they also perform their own assembly and maintenance. In human heart tissue, the mitochondrial membrane is composed of 18% cardiolipin, 34% phosphatidylethanolamine, 43% phosphatidylcholine, and 5% phosphatidylinositol (48). The mitochondrion can synthesize cardiolipin from phosphatidylglycerol and phosphatidylethanolamine from phosphatidylserine decarboxylation (48, 49). Phosphatidylserine is believed to be synthesized on the endoplasmic reticulum membrane closely associated with the mitochondria (49–51). The objective function representing the phospholipid synthesis activity of the mitochondria, $Z = 0.18$ cardiolipin + 0.34 phosphatidylethanolamine + 0.43 phosphatidylcholine, does not include phosphatidylinositol, because it is primarily produced in the endoplasmic reticulum (48). This objective function is used for the flux variability computations presented below.

Reactive Oxygen Species Detoxification—It has been reported that at least 2–5% of electrons transported on the electron transport chain are "lost" and therefore are not used to reduce oxygen to water (52). The lost electrons react with oxygen, hydroxide ions, nitrogen containing compounds, and fatty acids to form reactive radicals. These radicals are collectively referred to as ROS. The current network accounts for the generation of superoxides (O_2^-) but not other species. Superoxide dismutase reduces superoxides to hydrogen peroxide (H_2O_2), which is converted to water by either catalase or glutathione peroxidase. The contribution of catalase to this function is believed to be minimal compared with that of glutathione peroxidase in heart mitochondria (53). The glutathione peroxidase enzyme and the glutathione cycle use NADPH to reduce H_2O_2 and therefore implicitly impose an energetic stress on the cell. Consequently metabolism of glucose produces 3% less ATP when 2% of electrons are lost and 7% less ATP when 5% of electrons are lost. Oxidation of palmitate produces 3 and 8% less ATP for these two conditions, respectively. Calculations in the rest of this paper assume a 2% electron loss overall.

Network Robustness and Flexibility—To better understand the robustness and flexibility of the reconstructed network in carrying out its metabolic functions, we calculated the flux variability (16) of each reaction and analyzed the properties of equivalent optimal flux distributions (15, 31) in the network.

Flux Variability Analysis—The flexibility of a particular reaction in the mitochondrial network depends on the metabolic function under consideration. Flux variability analysis determines the allowable range of flux values while the network optimally satisfies a particular metabolic objective and physiological constraints on enzymatic capacities (Table III and Supplementary data S2).

When ATP production is considered to be the metabolic objective, the network has the least flexibility. Under this condition, only 8% of the 189 reactions have variable fluxes, 25% always have a constant non-zero flux value, and 67% are never used. Under heme synthesis condition, higher flexibility is observed with 60% reactions with variable fluxes, 8% have a constant non-zero flux, and 32% are not used. For phospholipid

TABLE V
Reaction participation among equivalent optimal flux distributions calculated with respect to the three metabolic objective functions

Optima refer to the extreme points of the solution space that achieve the optimal value for the objective function, whereas feasible extreme points only satisfy the constraints of the linear programming problem (see "Materials and Methods").

	ATP	Heme	Phospholipids
Total number of optima	4	8,288	21,863
Average reactions used per optimal solution	57.5	78.7	98.1
Reactions with variable fluxes	15	114	114
Reactions with constant (non-zero) fluxes	47	14	21
Reactions always used (largest correlated set)	53	35	56
Reactions never used	127	61	54
Number of feasible extreme points	9,160	11,000	50,012

synthesis, these proportions are 60, 11, and 29%, respectively. These results are summarized in Table V.

Among the reactions that have variable fluxes, the average flux ranges while maximizing for ATP, heme, and phospholipids are 60, 23, and 23 μmol/min/g proteins, respectively. Heme and phospholipid syntheses have the same set of reactions with variable fluxes. This set contains 114 reactions participating in glycolysis, citric acid cycle, OxPhos, β-oxidation, ROS detoxification, and the urea cycle (Supplemental data S3). Notably, it does not include any reactions in the heme and phospholipid synthesis pathways. 15 of these 114 reactions also have variable fluxes under the ATP synthesis condition. These 15 reactions are involved in catabolism (ATPS4m, PYK, PCm, PEPCKm, and NDPK1), phospholipid metabolism (DAGKm, and PAPAm), and transport (CITtam, CITtbm, GTPtm, HCO3Em, Htm, MALtm, PIt2m, and PYRt2m).

The flux range of reactions in the network when no objective function was imposed was also calculated for comparison (Fig. 1). These flux ranges are only slightly larger than the variation found when heme and phospholipids are optimized but are significantly higher than the ATP case. This implies that a large portion of the solution space is accessible for optimal heme and phospholipid syntheses, but it is much more restricted for ATP production.

Overall, in addition to transport reactions, those in glycolysis, the citric acid cycle, and OxPhos have the highest flux variability. Their flux variations across the three metabolic objectives can be visualized in Fig. 2. All reactions and their flux ranges can be found in the Supplemental data S3.

Properties of Alternate Optima—The number of different paths (equivalent flux distributions) that can optimally satisfy a metabolic function can be used to measure the robustness of a network. Similar to flux variability analysis, the number of alternative network flux distributions is a function of the metabolic objective and metabolite uptake rate (V_{max} of transporters). These constraints are the same as those used for flux variability analysis (Table III and supplementary S2).

When glucose, fatty acids, and glutamate were simultaneously available to produce ATP, only four (basic) optimal flux distributions were found. The average number of reactions used per optimal solution is 57.5 with a minimum of 55 and a maximum of 62 reactions (Table V). When the network was optimized for protoheme, a total of 8,288 equivalent flux distributions were found. On average, there are 78.7 reactions used per alternate optima ranging from 53 to 81 reactions. However, the network appears to be much more flexible in synthesizing phospholipids as compared with the other two cases. A large number of optimal flux distributions (21,863) were discovered. An average of 98.1 reactions were used across these flux distributions with a minimum of 75 and a maximum of 118.

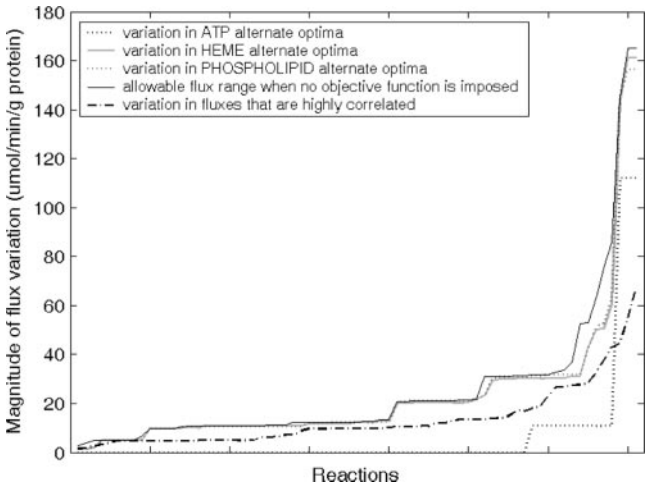

FIG. 1. **Ranges of flux variation (ordered by magnitude) found among flux distributions that are optimal for each metabolic objective function and among flux distributions that are highly correlated with each other.** The allowable flux ranges when no objective function is imposed is shown for comparison. Values on the *y* axis indicate the magnitude of flux variation (μmol/min/g proteins) observed for a particular reaction. There are 50 reactions between major tick marks on the *x* axis. For clarity the hundred reactions with the smallest flux variations have been omitted. Reaction Htm with flux variation higher than 400 is also omitted.

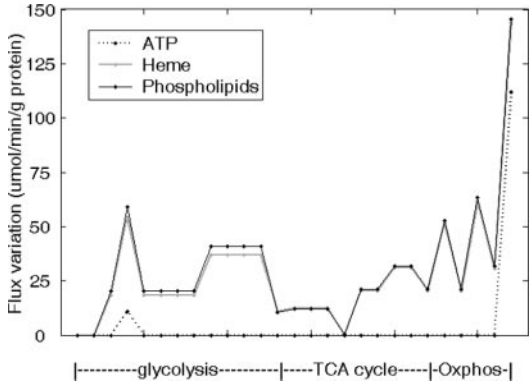

FIG. 2. **Ranges of flux variation (μmol/min/g proteins) found for reactions in glycolysis, the citric acid (*TCA*) cycle, and oxidative phosphorylation when the network produces maximal ATP, heme, and phospholipids.** The ordering of reactions on the *x* axis follows the order of reactions in these pathways (see Supplemental data S1). Larger allowable variations, hence higher network flexibility, were observed for maximal heme and phospholipid syntheses. Completed results of flux variability analysis can be found in Supplemental data S3.

Optimal Flux Distributions Are Correlated with Each Other—For each alternate optima associated with ATP production, we calculated its pairwise correlation with every heme and phospholipid alternate optima to determine the similarity between these flux distributions. Fig. 3, *a* and *b*, shows the cumulative distribution of correlation coefficients *r* between ATP and heme optimal fluxes and between ATP and phospholipid optimal fluxes. Both of these distributions share the same general characteristics. There are no pairs of fluxes with negative correlations. Roughly half of the pairs of fluxes have very low correlation ($r < 0.2$), and the other half have a very high correlation ($r > 0.9$). The absence of negative correlation among these fluxes suggests that when the mitochondrion is producing ATP for the cell, it is also likely to produce other compounds important for its own maintenance.

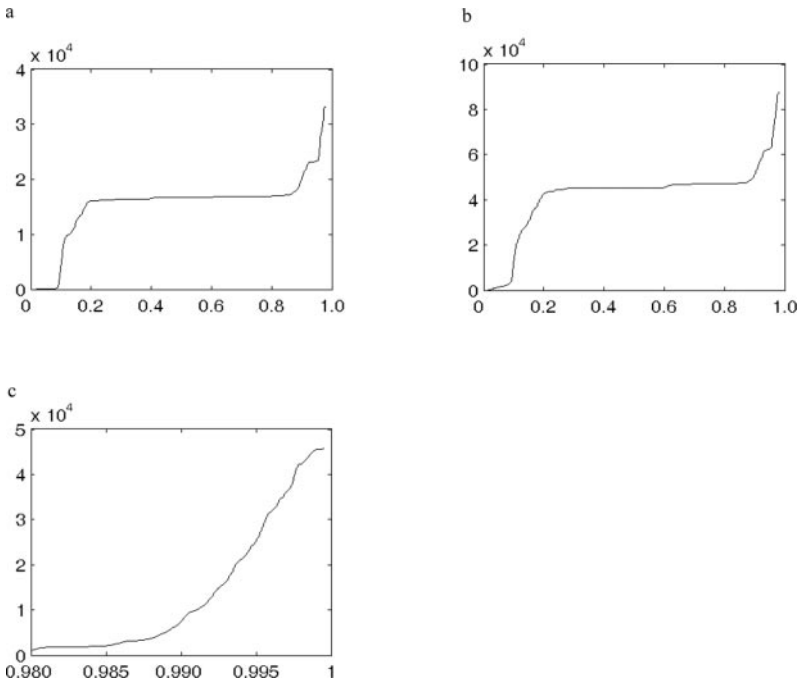

FIG. 3. **Cumulative distribution of correlation coefficients found between pairwise flux distributions.** *a*, ATP and heme optimal flux distributions. *b*, ATP and phospholipid optimal flux distributions. *c*, highly correlated heme and phospholipid flux distributions. Values on the *x* axis are Pearsons correlation coefficients. Each point on the plot corresponds to a particular pairing of two flux distributions.

We subsequently investigated the correlation among the sets of heme and phospholipid flux distributions that have very high correlations with ATP alternate optima ($r > 0.975$). Pairwise correlation between these fluxes was calculated (Fig. 3*c*). These flux distributions are very well correlated with each other; the majority have correlation values higher than 0.99. Using this criterion ($r > 0.99$), we identified a subset of 425 flux distributions (of a total of 30,155 alternate optima calculated) that are highly correlated with each other. One of the 425 flux distributions is an ATP optimal solution, 157 are heme optimal solutions, and the rest (267) are phospholipid optimal solutions.

In comparing the three flux distributions for ATP, heme, and phospholipid production that are most correlated with one another, we found that only 20 reactions need to be activated for the network to produce phospholipids and ATP simultaneously. Another seven reactions were needed for the syntheses of all three products. If it can be assumed that these three metabolic demands often take place simultaneously in the cell, then the subset of alternate optima that are highly correlated with one another are perhaps the most probable *in vivo* fluxes. Fig. 1 shows the flux variations (results of flux variability analysis) found among flux distributions that are optimal for individual metabolic objective functions and among those that are highly correlated with each other. The variation found in the latter case substantially reduces the flux range seen among heme and phospholipid optimal fluxes.

Distribution of Fluxes and Resources among the Three Mitochondrial Functions—We used multiple-objective analysis to investigate how the network distributes its resources to simultaneously satisfy all three metabolic functions. The lexicographic method allows one to hierarchically order the three objective functions. As we wanted to study the relative importance of each of the three functions, all six possible orderings were explored. In our experiments, all of the alternative optima for maximizing ATP demand have zero flux values for heme and phospholipids, so all four of these optimal extreme points are in the efficient frontier. Note that we could not achieve maximal value for either heme or phospholipid production when ATP output to the cytosol is at its optimal value (Table VI).

When the synthesis of either heme or phospholipids was maximized first, nearly optimal values were obtained for the other two functions. In fact, both heme and phospholipid productions achieve their maximum values simultaneously if ATP demand is strictly less than its maximum value (Table VI).

Similar results were observed using the weight formulation. In particular, we let $w = (g/(2 + g), 1/(2 + g), 1/(2 + g))$, where $g/(2 + g)$ corresponds to the weight coefficient of the ATP objective function, $1/(2 + g)$ corresponds to heme, and the last $1/(2 + g)$ corresponds to phospholipids. This allows us to assign equal weights to heme and phospholipid syntheses while varying the weight on ATP demand from $g = 0$ to $g = 20$. As g increases, the weight for ATP demand increases toward one. The composite objective begins with a simple average of heme and phospholipids, both at their maximum values of 0.125 and 3.704, respectively (Fig. 4*a*). For $g \geq 0.72$, the value of ATP demand reaches its maximum and heme and phospholipid biosyntheses both hold at zero (Fig. 4*b*).

However, the value of the composite objective function is biased by the metabolic function with dominant flux output (ATP production). To remove this bias, we rescaled the weight coefficient of each of the metabolic functions by its respective optimal flux value and then varied g such that w_1 goes from zero to approximately one. The value of this new composite objective function increases linearly with g.

The fact that both heme and phospholipid biosyntheses can be simultaneously maximized suggests that these two functions of the mitochondria can operate relatively independent from each other without affecting one another's resource pool. However, these two functions require energy in the form of ATP, thus reducing the available ATP for the cell. We do not view this as a compromise to the energy conversion ability of the mitochondria, because ATP is produced precisely for the purpose of fueling cellular processes both outside and inside the mitochondria.

Correlated Reaction Sets Form Network Modules—The sets of reactions that are always used together across all of the optimal flux distributions are referred to as correlated reaction sets (30, 54). These reactions form functional modules that are likely to be co-regulated. Correlated reaction sets among optimal solutions calculated for each objective function and among

TABLE VI
Results of multiple-objective analysis using the lexicographic method

Each permutation shows the order for which the three objective functions are optimized: (A) ATP; (H) Heme; and (P) Phospholipids. Each column contains the maximal value achieved for one particular objective function given its position in the permutation. These values are normalized by the network's maximal output of the corresponding metabolic function when the other two functions are not considered.

Permutation	ATP	Heme	Phospholipids
A-H-P	1	0	0
A-P-H	1	0	0
H-A-P	0.92	1	0.06
H-P-A	0.75	1	1
P-A-H	0.81	0	1
P-H-A	0.75	1	1

highly correlated flux distributions were identified (see Supplemental data S4 and S5A).

Reactions that are always active with respect to a specific objective function form the largest correlated reaction set under that objective function. Therefore, under the three objective functions (ATP production, heme synthesis, and phospholipid synthesis), the largest correlated reaction sets contain 53, 35, and 56 reactions, respectively (Table V).

When ATP production was used as the objective function, two more correlated reaction sets were found. One set contains DPK1 and GTPtm, which participate in the conversion of GPT produced by substrate level phosphorylation to ATP. The other reaction set uses phosphoenolpyruvate kinase (PEPCKm) to consume GTP (and oxaloacetate) to produce phosphoenolpyruvate. Two of the four ATP optimal flux distributions use NDPK1 and GTPtm. These two flux distributions were found to be much better correlated with heme and phospholipid optima, which confirms that mitochondria usually convert GTP to ATP directly.

When heme and phospholipid syntheses were used as the objective functions, 19 and 13 other correlated reaction sets were found, respectively (Supplemental data S4 and S5A). Some of these correlated sets are present in both cases. Two of these sets contain reactions in the urea cycle and glycolysis. One of these sets appears to form a module for oxygen metabolism. Seven other sets contain reactions involved in shuttling and oxidation of the seven fatty acids. The remaining sets are smaller with two or three reactions each. Reactions within each of these sets are also known to be involved in the same biochemical pathway.

Correlated reaction sets found among highly correlated flux distributions form functional modules that nicely encompass reactions known to participate in the same or connected biochemical pathways. In particular, we found reaction sets corresponding to lipid metabolism, heme biosynthesis, glycolysis, citric acid and OxPhos, urea cycle, and Mal/Asp shuttle (Supplemental data S4). These results show that given fluxomic data, this method can be used to identify functional modules that represent physiologically significant components in the network.

Distribution of Flux Values among the Equivalent Optimal Flux Distribution—The distribution of flux values of a reaction across all of the equivalent optimal solutions can be interpreted as the activity profile of that reaction. These profiles are analogous to gene expression profiles, but they represent enzyme activity levels rather than mRNA transcript levels.

Because most reactions under maximal ATP production conditions do not have much flux variation, only profiles for the heme and phospholipid syntheses are discussed further. Profiles of reactions in glycolysis, the citric acid cycle, and OxPhos for heme and phospholipid biosyntheses are shown in Fig. 5. In general, the uses of these reactions are similar in both cases. Glycolytic reactions have a bimodal distribution with high peak values at extreme ends of the flux range, *i.e.* either these reactions are fully used or not at all in the optimal solutions. The citric acid cycle reactions have more diverse distributions (Fig. 5). Also, reactions corresponding to complexes I and II seem to have a broader distribution of flux values than the rest of the reactions of the electron transport chain.

Flux distribution profiles of reactions in the urea cycle, ROS detoxification, and fatty acid metabolism are nearly identical for both the heme and phospholipid synthesis cases (Supplemental data S5B and S5C). Reactions in the urea cycle and ROS detoxification pathway tend to have one or two dominant flux values with a few reactions having no variation. Reactions in fatty acid transport and oxidation all have two major peaks at extreme ends of the flux spectra with the exception of the carnitine carrier (CRNtim). These profiles suggest that only a subset of the six fatty acids types is used one at a time by the network. However, since the carnitine carrier is shared among all of the long-chain fatty acids, it tends to be active regardless of which fatty acid is used. The rest of the reactions in the network do not have much variation.

DISCUSSION

This study presents a comprehensive reconstruction and characterization of the mitochondrial metabolic network in human cardiomyocytes based on proteomic and biochemical data from scientific literature. Thus this reconstruction accounts for mitochondrial functions other than energy metabolism. The key results of this study are as follows. 1) The systemically determined ATP yield per glucose is 31.5. 2) The network has high flexibility for maximal biosynthesis of heme and phospholipids but modest flexibility for maximal ATP production. 3) A subset of optimal flux distributions is highly correlated with each other and thus is the most probable *in vivo* fluxes. 4) The correlated reaction sets found from alternate optima define functional modules in the network.

The present reconstruction of the mitochondrial network represents the integration and simultaneous analysis of heterogeneous data types. Systemic analysis of the three mitochondrial metabolic objectives highlights the interdependence of various biochemical pathways in this organelle. Oxidative phosphorylation fulfills the energetic requirement for heme and phospholipid syntheses, whereas the latter processes provide the maintenance for proteins and membrane structure essential for the energy conversion pathway. Furthermore, as the mitochondrial metabolism undoubtedly influences its signaling and regulatory roles in the cell, this reconstruction provides a basis that can be extended to study other less characterized mitochondrial processes. Such iterative network reconstruction to expand the scope and capabilities of *in silico* models has been performed for *Escherichia coli* (55) and yeast (56).

Mitochondria constitute up to 35% of the mammalian cardiac myocyte volume (53). The primary function of cardiac mitochondria is to produce energy for the contraction of the heart. Therefore, it is likely that these mitochondria can operate close to the theoretical metabolic limits. The complete mitochondrial network reconstruction allows for a systemic (*i.e.* on a network wide basis) and accurate calculation of the allowable ATP yields and P/O ratios from the oxidation of various metabolites. The present network produces the net Reaction 1 from glycolysis,

$$\text{Glucose} + 2\ P_i + 2\ \text{ADP} + 2\ \text{NAD} \rightarrow 2\ \text{pyruvate} + 2\ \text{ATP} + 2\ \text{NADH} + 2\ H^+ + 2\ H_2O$$

REACTION 1

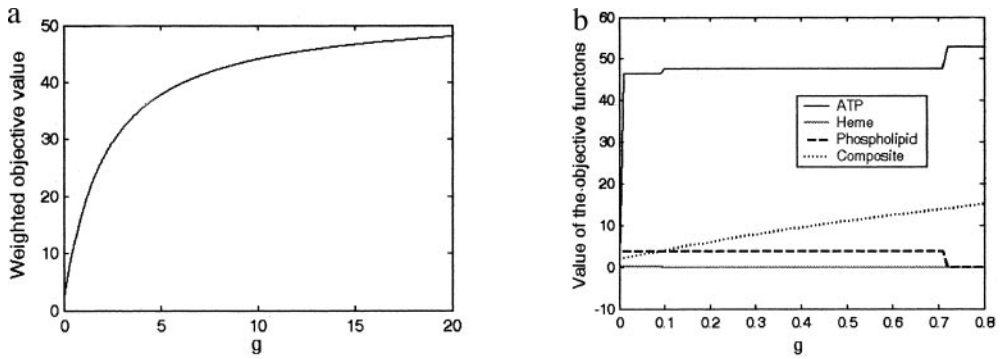

FIG. 4. **Results of multiple-objective analysis using the weight method.** *a*, value of the composite objective function (μmol/min/g proteins) increases as more weight is put on the production of ATP by increasing g. Each point on the plot indicates the optimal value of the weighted objective function calculated for a specific value of g. The three metabolic functions are weighed such that ATP synthesis has a weight coefficient of g/(2 + g) and heme and phospholipids are weighed equally with 1/(2 + g). *b*, value of the composite and individual objective functions (μmol/min/g proteins) as a function of g. For values of g > 0.72, the syntheses of both heme and phospholipids equal zero and the production of ATP achieves its maximal value.

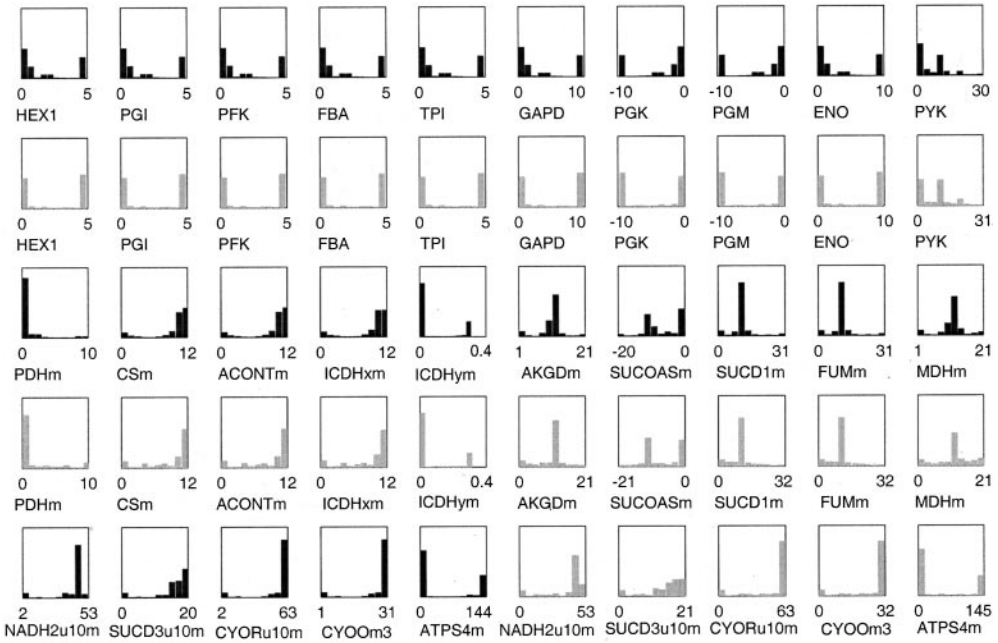

FIG. 5. **Distribution of flux values for reactions in glycolysis, the citric acid cycle, and oxidative phosphorylation among equivalent optimal flux distributions.** The figures colored in *gray* correspond to the case where phospholipid synthesis is the objective function. The *black figures* correspond to the case where heme synthesis is the objective function. Values on the *x* axes denote the minimum and maximum flux values the corresponding reaction can undertake. *y* axes have values from 0 to 1, denoting the probability of a particular flux value. See Supplemental data S1 for reaction abbreviations.

which agrees with most biochemistry textbooks (40, 41). Nevertheless, existing calculations of ATP yield on glucose do not account for the fate of the protons produced in the preceding net reaction in computing the overall ATP yield by glucose. These protons must be consumed when one considers a network-wide proton balance. Considering the high rate of glycolysis taking place in muscle cells, the generated protons probably affect the mitochondrial intermembrane gradient, thus contributing to ATP production in the mitochondria.

Although the mitochondria of different tissues tend to specialize in specific functions, the three metabolic functions described in this paper are shared among mitochondria of most tissues. As the demand for these three functions are likely to be simultaneous, it would not be surprising that the mitochondria use similar sets of reactions to meet all three demands. This reduces the number of candidate flux distributions by two orders of magnitude. It is expected that, as more objective functions (corresponding to additional mitochondrial functional roles) are formulated, we will be able to narrow down and therefore identify with higher confidence the reaction fluxes in the network.

The alternate optima reported in this study were calculated with respect to one objective function at a time while setting the other two functions to zero. This approach was done so that we could enumerate equivalent metabolic pathways that maximally satisfy one metabolic function without being influenced by reactions that are used for a different metabolic objective. It also eliminated pathways that used unnecessarily high numbers of reactions only to produce by-products that were not part of the objective function. The drawback was that we missed extreme points that simultaneously produce all three metabolic products: ATP, heme, and phospholipids. Our effort to enumerate all of the alternate optima without setting two objective functions to zero has been computationally infeasible within practical time. Nevertheless, among the alternate optima that we found, those that are highly correlated with each other give us clues regarding the flux distributions that simultaneously satisfy all three metabolic functions.

Within a set of alternate optima, reactions that always appear together (correlated reaction sets) can be identified. The correlated reaction sets identified for the present mitochondrial network clearly show that they form functional modules within the network. Whether or not enzymes within these functional modules actually share the same regulatory mechanism is perhaps a more difficult question to answer. Since most of these enzymes are encoded in the nuclear genome and many of them are post-transcriptionally regulated, co-appearance inside the mitochondria may not directly imply co-expression in the nucleus. Nevertheless, knowledge regarding these functional modules allows us to better understand how the separate components in the network function to carry out the objectives of the entire mitochondrion.

In summary, we have reconstructed the most complete metabolic network of the human mitochondrion to date. The initial analysis of this reconstruction allows the evaluation of optimal functionalities such as systemic ATP yields and assessments of network flexibility. This study represents the first step toward the generation of a biochemically structured framework within which the systemic properties of the mitochondria can be studied. Moreover, as additional high throughput data (*i.e.* metabolomic, isotopomer, and sequence variation data) become available, this reconstruction can serve as a model-centric database to evaluate and reconcile these diverse datasets as well as using them to improve model predictions.

Acknowledgments—We thank Jennifer Reed and Nathan Price for their help with the characterization of the alternate optima and preparation of this paper as well as Dr. Robert Naviaux for advice on mitochondrial biology.

REFERENCES

1. Vu, T. H., Hirano, M., and DiMauro, S. (2002) *Neurol. Clin.* **20,** 809–839
2. Santos, D. L., Palmeira, C. M., Seica, R., Dias, J., Mesquita, J., Moreno, A. J., and Santos, M. S. (2003) *Mol. Cell. Biochem.* **246,** 163–170
3. Carew, J. S., and Huang, P. (2002) *Mol. Cancer*, www.molecular-cancer.com/content/1/1/9
4. Anderson, S., Bankier, A. T., Barrell, B. G., de Bruijn, M. H., Coulson, A. R., Drouin, J., Eperon, I. C., Nierlich, D. P., Roe, B. A., Sanger, F., Schreier, P. H., Smith, A. J., Staden, R., and Young, I. G. (1981) *Nature* **290,** 457–465
5. Ozawa, T., Sako, Y., Sato, M., Kitamura, T., and Umezawa, Y. (2003) *Nat. Biotechnol.* **21,** 287–293
6. Taylor, S. W., Fahy, E., Zhang, B., Glenn, G. M., Warnock, D. E., Wiley, S., Murphy, A. N., Gaucher, S. P., Capaldi, R. A., Gibson, B. W., and Ghosh, S. S. (2003) *Nat. Biotechnol.* **21,** 281–286
7. Verma, M., Kagan, J., Sidransky, D., and Srivastava, S. (2003) *Nat. Rev. Cancer* **3,** 789–795
8. Sherry, A. D., Jeffrey, F. M., and Malloy, C. R. (2004) *Metab. Eng.* **6,** 12–24
9. Covert, M. W., Schilling, C. H., Famili, I., Edwards, J. S., Goryanin, I. I., Selkov, E., and Palsson, B. O. (2001) *Trends Biochem. Sci.* **26,** 179–186
10. Palsson, B. O. (2000) *Nat. Biotechnol.* **18,** 1147–1150
11. Edwards, J. S., and Palsson, B. O. (2000) *BMC Bioinformatics* www.biomedcentral.com/1471-2105/1/1
12. Kauffman, K. J., Prakash, P., and Edwards, J. S. (2003) *Curr. Opin. Biotechnol.* **14,** 491–496
13. Papin, J. A., Price, N. D., Edwards, J. S., and Palsson, B. O. (2002) *J. Theor. Biol.* **215,** 67–82
14. Price, N. D., Papin, J. A., and Palsson, B. O. (2002) *Genome Res.* **12,** 760–769
15. Lee, S., Phalakornkule, C., Domach, M. M., and Grossmann, I. E. (2000) *Comp. Chem. Eng.* **24,** 711–716
16. Mahadevan, R., and Schilling, C. H. (2003) *Metab. Eng.* **5,** 264–276
17. Edwards, J. S., Ramakrishna, R., Schilling, C. H., and Palsson, B. O. (1999) in *Metabolic Engineering* (Lee, S. Y., and Papoutsakis, E. T., eds) pp. 13–57, Marcel Dekker, Inc., New York
18. Bonarius, H. P. J., Schmid, G., and Tramper, J. (1997) *Trends Biotechnol.* **15,** 308–314
19. Rocquelin, G., Guenot, L., Astorg, P. O., and David, M. (1989) *Lipids* **24,** 775–780
20. Gloster, J., and Harris, P. (1970) *J. Mol. Cell. Cardiol.* **1,** 459–465
21. Gloster, J., and Harris, P. (1969) *Cardiovasc. Res.* **3,** 45–51
22. Genomatica. (2003) *Sympheny*, San Diego, CA
23. Schilling, C. H., Letscher, D., and Palsson, B. O. (2000) *J. Theor. Biol.* **203,** 229–248
24. Price, N. D., Famili, I., Beard, D. A., and Palsson, B. O. (2002) *Biophys. J.* **83,** 2879–2882
25. GAMS Development Corporation (2003) *GAMS*, 21.1 Ed., Washington, D. C.
26. Anderson, E. D. (2002) *Mosek ApS*, Copenhagen, Denmark
27. The MathWorks, Inc. (2003) *MATLAB*, The MathWorks, Inc., Natick, MA
28. Avis, D. (2000) in *Polytopes-Combinatorics and Computation* (Kalai, G., and Ziegler, G., eds) Vol. 29, pp. 177–198, Birkhauser-Verlag
29. Avis, D. (2003) *Irs*, cgm.cs.mgill.ca/~avis/C/Irs.html
30. Papin, J. A., Price, N. D., and Palsson, B. O. (2002) *Genome Res.* **12,** 1889–1900
31. Phalakornkule, C., Lee, S., Zhu, T., Koepsel, R., Ataai, M. M., Grossmann, I. E., and Domach, M. M. (2001) *Metab. Eng.* **3,** 124–137
32. Westermann, B., and Neupert, W. (2003) *Nat. Biotechnol.* **21,** 239–240
33. Danial, N. N., Gramm, C. F., Scorrano, L., Zhang, C. Y., Krauss, S., Ranger, A. M., Datta, S. R., Greenberg, M. E., Licklider, L. J., Lowell, B. B., Gygi, S. P., and Korsmeyer, S. J. (2003) *Nature* **424,** 952–956
34. Voet, D., Voet, J. G., and Pratt, C. W. (1999) *Fundamentals of Biochemistry*, John Wiley & Sons, Inc., New York
35. Aimar-Beurton, M., Korzeniewski, B., Letellier, T., Ludinard, S., Mazat, J. P., and Nazaret, C. (2002) *Mol. Biol. Rep.* **29,** 227–232
36. Cortassa, S., Aon, M. A., Marban, E., Winslow, R. L., and O'Rourke, B. (2003) *Biophys. J.* **84,** 2734–2755
37. Korzeniewski, B., and Mazat, J. P. (1996) *Biochem. J.* **319,** 143–148
38. Ramakrishna, R., Edwards, J. S., McCulloch, A., and Palsson, B. O. (2001) *Am. J. Physiol.* **280,** R695–R704
39. Searcy, D. G. (2003) *Cell Res.* **13,** 229–238
40. Salway, J. G. (1999) *Metabolism at a Glance*, 2nd Ed., Blackwell Science, Malden, MA
41. Stryer, L. (1995) *Biochemistry*, 4th Ed., W. H. Freeman, New York
42. Grynberg, A., and Demaison, L. (1996) *J. Cardiovasc. Pharmacol.* **28,** Suppl. 1**,** S11–S17
43. Rocquelin, G., Guenot, L., Justrabo, E., Grynberg, A., and David, M. (1985) *J. Mol. Cell. Cardiol.* **17,** 769–773
44. Lehninger, A. L., Cox, M. M., and Nelson, D. L. (1993) *Principles of Biochemistry*, 2nd Ed., Worth Publishers, New York, NY
45. Atamna, H., Walter, P. B., and Ames, B. N. (2002) *Arch. Biochem. Biophys.* **397,** 345–353
46. Sedman, R., Ingall, G., Rios, G., and Tephly, T. R. (1982) *Biochem. Pharmacol.* **31,** 761–766
47. Edwards, J. S., Ramakrishna, R., and Palsson, B. O. (2002) *Biotechnol. Bioeng.* **77,** 27–36
48. Daum, G. (1985) *Biochim. Biophys. Acta* **822,** 1–42
49. Shiao, Y. J., Lupo, G., and Vance, J. E. (1995) *J. Biol. Chem.* **270,** 11190–11198
50. Stone, S. J., and Vance, J. E. (2000) *J. Biol. Chem.* **275,** 34534–34540
51. Vance, J. E. (1990) *J. Biol. Chem.* **265,** 7248–7256
52. Brown, G. C., Nicholls, D. G., and Cooper, C. E. (1999) *Mitochondria and Cell Death*, Princeton University Press, Princeton, NJ
53. Antunes, F., Han, D., and Cadenas, E. (2002) *Free Radic. Biol. Med.* **33,** 1260–1267
54. Burgard, A. P., Nikolaev, E. V., Schilling, C. H., and Maranas, C. D. (2004) *Genome Res.* **14,** 301–312
55. Reed, J. L., Vo, T. D., Schilling, C. H., and Palsson, B. O. (2003) *Genome Biol.* **4,** R54.51–R54.12
56. Duarte, N. C., Herrgard, M. J., and Palsson, B. O. (2004) *Genome Res.* **14,** 1298–1309
57. Indiveri, C., Tonazzi, A., and Palmieri, F. (1991) *Biochim Biophys Acta* **1069,** 110–116
58. Murthy, M. S., and Pande, S. V. (1984) *J. Biol. Chem.* **259,** 9082–9089
59. Williamson, J. R., Hoek, J. B., Murphy, E., Coll, K. E., and Njogu, R. M. (1980) *Ann. N. Y. Acad. Sci.* **341,** 593–608
60. Bunger, R., and Mallet, R. T. (1993) *Biochim. Biophys. Acta* **1151,** 223–236
61. Palmieri, L., Pardo, B., Lasorsa, F. M., del Arco, A., Kobayashi, K., Iijima, M., Runswick, M. J., Walker, J. E., Saheki, T., Satrustegui, J., and Palmieri, F. (2001) *EMBO J.* **20,** 5060–5069
62. Claeys, D., and Azzi, A. (1989) *J. Biol. Chem.* **264,** 14627–14630
63. Fiermonte, G., Dolce, V., Arrigoni, R., Runswick, M. J., Walker, J. E., and Palmieri, F. (1999) *Biochem. J.* **344,** 953–960
64. Fiermonte, G., Dolce, V., David, L., Santorelli, F. M., Dionisi-Vici, C., Palmieri, F., and Walker, J. E. (2003) *J. Biol. Chem.* **278,** 32778–32783
65. De Marcos Lousa, C., Trezeguet, V., Dianoux, A. C., Brandolin, G., and Lauquin, G. J. (2002) *Biochemistry* **41,** 14412–14420